

Comparison of atomic potentials and eigenvalues in strongly coupled neon plasmas

R. Cauble

Berkeley Research Associates, Springfield, Virginia 22151

M. Blaha

Laboratory for Plasma and Fusion Energy Studies, University of Maryland, College Park, Maryland 20742

J. Davis

Naval Research Laboratory, Washington, D.C. 20375

(Received 26 October 1983)

A self-consistent, completely-quantum-mechanical formalism has been developed that characterizes the fundamental atomic properties of ions in dense plasmas. This theory is applied to neon plasmas under strongly coupled conditions and the results are compared with those obtained from the hypernetted-chain approximation employing a semiclassical two-body interaction. The comparisons point out the lack of validity of simple approximations for atomic calculations in strongly coupled plasmas and indicate that the self-consistent theory provides a method of obtaining meaningful results even when the plasma ion coupling parameter is of order 5.

I. INTRODUCTION

Since it is now possible to produce very hot plasmas at greater than solid density in the laboratory, it is meaningful to construct theoretical models of such systems that allow for accurate determination of the systems' properties. For calculations of atomic properties the usual approach is to iteratively solve a set of coupled equations statistically describing the charge distributions and an effective electron-ion interaction potential. Incorporating this potential, the bound- and free-electron distributions are found from the Schrödinger equation. Thus, given an ion where the bound orbits are not externally specified, the solution of the equations directly gives orbital energy eigenvalues and (fractional) populations. The wave functions and the effective electrostatic potential obtained in this manner can be used to find spontaneous decay rates and cross sections for various atomic processes characterizing radiation, the spectrum of which can be employed to diagnose the plasma environment.^{1,2}

Thomas-Fermi and Hartree-Fock statistical models have been applied to highly ionized atoms in dense plasmas^{3,4} and subsequently applied to a strongly coupled neon plasma.² However, ion correlations were neglected in these approaches. A self-consistent set of Schrödinger-Poisson equations including ion correlations was developed by Skupsky⁵ to study the plasma microfield effects on a high- Z impurity ion embedded in a dense fully ionized low- Z plasma. An improvement over this method—the quantum-mechanical treatment of the free electrons—was made by Davis and Blaha.⁶ In a similar manner, density-functional theory (DFT) has been employed to investigate level shifts and screening effects in the impurity problem.^{7,8}

The inclusion of ion correlations in these latter models is accomplished using a Boltzmann distribution under the assumption of nearly classical ion interactions. In the

case of the one-component plasma (dynamic ions in a neutralizing background charge), the assumption of a Boltzmann-like form for the ions would be erroneous for values of the ion coupling parameter

$$\Gamma = \frac{(\bar{Z})^2 e^2 \beta}{r_0}$$

greater than about three.^{9,10} Here \bar{Z} is the effective ionic charge, r_0 is the ion-sphere radius, and $\beta = 1/k_B T$. This discrepancy is not as significant for a “real” two-species plasma because the mobile electron fluid is able to provide more effective screening, but has yet to be investigated in the two-species model for $\Gamma > 2$ and for ions other than hydrogen. If one can utilize a model that is expected to provide accurate distributions for a strongly coupled system, one can also use that model to examine the validity of using self-consistent statistical models in the strongly coupled regime.

Implicit in all the methods discussed here is the assumption that the lifetime of the ionic state is long enough so that the plasma has time to be polarized by the ion. Since the polarization (correlation) time is of the order of the inverse of the plasma frequency, all of the cases we are considering can be considered long-lived (a typical state lifetime—the most rapid destruction mechanism being collisional deexcitation—may be of the order of 10^{-14} – 10^{-15} s; ω_p^{-1} is about 10^{-17} s). Each model also assumes that since the ion state exists through many plasma periods, the concept of a time-averaged potential for atomic calculations is meaningful.

It should be noted that the calculations involving the self-consistent method presented below, like those of Ref. 8, form an “average atom” ion model, in contrast with models which detail the ionic configuration. The eigenenergies obtained below do not represent the spectrum of an ion in a specific configuration (i.e., hydrogenic), but

represent an average over many ions in partially ionized states.

We investigate here the energy eigenvalues, charge distributions, and effective electron-ion potentials for strongly coupled neon plasmas using a self-consistent DFT model similar to that described in Ref. 8. These results are compared with those obtained from the solution of the two-component plasma hypernetted-chain (HNC) equations, which are assumed to be valid at these densities and temperatures. The results will indicate the inadequacy of the Debye-Hückel (DH) and ion-sphere (IS) calculations when $13 < \Gamma < 1$.

In Sec. II we describe the atomic and plasma models we will consider. Section III contains the results of computations employing these models. The results are discussed in the concluding section.

II. MODELS

We consider an ion of nuclear charge Z in a plasma in which the average effective charge is \bar{Z} . \bar{Z} is equal to Z minus the mean number of bound electrons per ion and is a result of the model. Density-functional theory leads to a system of equations that must be solved self-consistently. The electrostatic potential is given by the Poisson equation

$$V(r) = \frac{Ze^2}{r} + 4\pi e^2 \left[\frac{1}{r} \int_0^r dr' r'^2 (\rho_e + \rho_b + \rho_i) + \int_r^\infty dr' r' (\rho_e + \rho_b + \rho_i) \right]. \quad (1)$$

The plasma is assumed to be in thermal equilibrium and all electrical charge distributions are assumed to be spherically symmetric. In Eq. (1), ρ_b is the local density of bound electrons

$$\rho_b = -(4\pi r^2)^{-1} \sum_{n,l} b_{nl} P_{nl}^2(r). \quad (2)$$

The b_{nl} are the state occupation numbers ($\sum_{nl} b_{nl} = Z - \bar{Z}$) and $P_{nl}(r)$ are the radial wave functions found from solving the Schrödinger equation where the interaction potential is $V(r)$ from Eq. (1) with ρ_b set equal to zero,

$$\left[\frac{d^2}{dr^2} - \frac{l(l+1)}{r^2} + V(r) - V_{xc}(r) - V_{xc}(\infty) + E_{nl} \right] P_{nl}(r) = 0, \quad (3)$$

where E_{nl} is the energy eigenvalue of state nl . Here, the exchange-correlation potential $V_{xc}(r)$ has been calculated by Gupta and Rajagopal¹¹ and by Dharma-wardana and Taylor.¹²

ρ_e is the local charge density of free electrons. It is represented by a Fermi-Dirac energy distribution beyond a spherical boundary large enough so that the plasma at the boundary may be considered neutral. Inside this sphere the free electrons may be treated quantum mechanically and are described by wave functions that are solutions of

the time-independent Schrödinger equation, i.e.,

$$\rho_e = - \int_0^\infty dr W(k) \frac{1}{k^2 r^2} \sum_{l=0}^\infty (2l+1) F_{kl}^2(r), \quad (4)$$

where

$$W(k) = \frac{k^2}{\pi^2} \left\{ 1 + \exp \left[\left[\frac{k^2}{2} - \mu \right] \beta \right] \right\}^{-1}; \quad (5)$$

here μ is the chemical potential of the free-electron gas determined from

$$\int_0^\infty dk W(k) = \rho_e(\infty) = -n_e, \quad (6)$$

where n_e is the mean electron density. The free-electron wave functions F_{kl} are solutions of Eq. (3) with the replacement of the eigenenergy E_{nl} by the electron kinetic energy k^2 . The ion charge density is assumed to take the Boltzmann form

$$\rho_i = \frac{n_e}{Z} e^{-\beta V(r)}. \quad (7)$$

At $r = \infty$, $\rho_i = -\rho_e$, ensuring neutrality; we also have the boundary conditions $rV(r) \rightarrow 0$ and $P_{nl} \rightarrow 0$ as r approaches infinity. Equations (1)–(4), (6), and (7) are solved self-consistently with these boundary conditions to yield E_{nl} , ρ_e , ρ_i , and $V(r)$. Details can be found in Ref. 6.

In order to gauge the reliability of the above model in a strongly coupled plasma, we turn to a semiclassical treatment of particle correlations that has been found to accurately reproduce molecular-dynamics calculations in this regime. In this approach—the two-component plasma (TCP)—the ions and electrons are treated as classical particles that interact through effective two-body potentials which deviate from pure Coulomb barrier at short distances such that the essential quantum diffraction effects are simulated. A particular form has been suggested by Deutsch¹³ and used in the computer simulations.¹⁴ This form uses the reduced mass de Broglie wavelength $\lambda_{\alpha\beta}$, where α and β are species labels, as a quantum-mechanical cutoff parameter, i.e.,

$$V_{\alpha\beta}(r) = \frac{\zeta_\alpha \zeta_\beta e^2}{r} [1 - \exp(-r/\lambda_{\alpha\beta})]; \quad (8)$$

ζ_α is the charge of species α , and $\lambda_{\alpha\beta} = \hbar / (2\pi \mu_{\alpha\beta} k_\beta T)^{1/2}$ where $\mu_{\alpha\beta}$ is the reduced mass. This potential is finite at the origin and is expected to give reasonable results for nondegenerate plasmas so long as $\lambda_{ee}/r_0 \ll 1$ (λ_{ee} is the smallest of the three $\lambda_{\alpha\beta}$). This condition is equivalent to $\Gamma < 9(\bar{Z})^2 / (T_{eV})^{1/2}$.

In order to include the plasma many-body effects, the binary interactions defined in Eq. (8) are used in the HNC equations.¹⁵ This is an approximate integral equation method for calculating static correlation functions for systems of particles with long-range potentials and has proven to be accurate for strongly coupled hydrogen plasmas.¹⁴ The quantities of interest are the radial distribution functions (RDF's) $g_{\alpha\beta}(r)$, which contain the static structural information in the TCP. The HNC approximation for the RDF's is

$$g_{\alpha\beta}(r) = \exp[-\beta V_{\alpha\beta}(r) + h_{\alpha\beta}(r) - c_{\alpha\beta}(r)], \quad (9)$$

where the total correlations

$$h_{\alpha\beta}(r) = g_{\alpha\beta}(r) - 1 \quad (10)$$

are related to the direct correlations $c_{\alpha\beta}$ by the Ornstein-Zernicke equations

$$\tilde{h}_{\alpha\beta}(k) = \tilde{c}_{\alpha\beta}(k) + \sum_{\gamma}^{i,e} h_{\alpha\gamma}(k) \tilde{c}_{\gamma\beta}(k). \quad (11)$$

Here the Fourier transform is defined as

$$\tilde{h}_{\alpha\beta}(k) = 4\pi n_{\alpha} \int_0^{\infty} dr r^2 \frac{\sin(kr)}{kr} h_{\alpha\beta}(r). \quad (12)$$

Equations (9)–(12) are solved iteratively for $\alpha, \beta = i, e$. The RDF's generated by this procedure reduce to their DH forms in the limit of weak coupling ($\Gamma \ll 1$), but are considerably different from the DH approximation when Γ is order 1 or larger.

The TCP is a model system of point charges, ions with charge $+\bar{Z}$ and free electrons with charge -1 . Formally the HNC scheme requires the exact \bar{Z} as an input parameter; this is necessary if the ionic and electronic distribution functions are to be examined. In order to find the effective potential, however, only a rough guess of \bar{Z} will suffice to determine much of the $V(r)$ curve.

If the particle distributions are required (therefore an accurate value of \bar{Z} is needed) two steps are necessary. First, a guess of \bar{Z} is made and the HNC equations are solved for $S_{ii}(k)$ and $S_{ie}(k)$. A "guess" of the potential is then found from Eq. (13) below. This potential can then be used in Eq. (3) to find wave functions for all bound states. The integrated wave functions provide a new \bar{Z} , which, when used in the HNC code a second time, provide a new potential and the needed distributions. Generally, only the one such iteration is required.

The effective electron-ion potential and the screening function $\tilde{\epsilon}^{-1}(k)$ are defined via Poisson's equation, the Fourier transform of which is given by

$$\tilde{V}_{\text{HNC}}(k) = \frac{4\pi e^2 \bar{Z}}{k^2 \tilde{\epsilon}(k)} = \frac{4\pi e^2 \bar{Z}}{k^2} [\tilde{S}_{ii}(k) - \tilde{S}_{ie}(k) / (\bar{Z})^{1/2}]. \quad (13)$$

The static structure factors are defined by

$$\tilde{S}_{\alpha\beta}(k) = \delta_{\alpha\beta} + (|\zeta_{\alpha}\zeta_{\beta}|)^{1/2} \tilde{h}_{\alpha\beta}(k). \quad (14)$$

The use of the nuclear charge Z in the definition of V_{HNC} requires some justification since the HNC charge distributions that make up $\tilde{S}_{\alpha\beta}$ are based on ions with charge \bar{Z} . This point is discussed in the Appendix.

The definition¹⁶ of $V(r)$ in Eq. (13) implies a form of the dielectric function significantly different from that obtained using the fluctuation-dissipation theorem¹⁷ (FDT), although both forms reduce to DH forms in the proper limits. For dense plasmas, V_{HNC} from Eq. (13) agrees much more closely with results from the ion-sphere model (described below) and with Thomas-Fermi² calculations, as well as the "potential of mean force" approximation $V_{\text{MF}}(r) = (Ze^2/r) \ln[g_{ei}(r)]$, than an effective interaction derived from the FDT. In fact, $V_{\text{FDT}}(r)$ shows screening that everywhere has a larger magnitude than

$V_{\text{DH}}(r)$. The Debye potential itself is known already to predict excessive screening in plasmas where the validity of the DH approximation is questionable. A plasma in a near metallic state (where the ion-sphere model might be used) shows a form very similar to the potential defined via Poisson's equation, which is qualitatively and quantitatively distinct from an effective interaction derived from the FDT. The IS model^{5,18} assumes complete ion shielding within an ion-sphere radius by a uniform cloud of electrons. Poisson's equation in this case yields

$$V_{\text{IS}}(r) = Ze^2 \left[\frac{1}{r} - \frac{1}{2r_0} \left[3 - \frac{r^2}{r_0^2} \right] \right]. \quad (15)$$

For extreme densities, V_{IS} should be approximately correct.

In this paper we compare a self-consistent density-functional atomic model with calculations gained via a solution of the two-component plasma HNC system of equations. We should mention that Dharma-wardana and Perrot¹⁹ have included an HNC scheme (for ions only) within a density-functional model in an effort to incorporate ion correlations. Their results for $g_{ii}(r)$ and $g_{ie}(r)$ compare favorably with molecular-dynamics results for fully ionized hydrogen.

III. RESULTS

We consider a strongly coupled neon gas plasma. Table I summarizes the conditions under which the runs were made, the value of \bar{Z} being a result of the self-consistent (SC) model. All cases have Γ 's in excess of 2. We note that both the HNC and SC models reduce to correct Debye-Hückel results in the limit of weak coupling ($\Gamma \ll 1$).

The ion charge density from the self-consistent model normalized to the background density, $\rho_i/\rho(\infty)$, is equivalent to the ion-ion radial distribution function g_{ii} . Figure 1 displays the ion distributions resulting from SC solutions for the $\Gamma = 2.2$ and 4.9 cases. These figures are compared with g_{ii} from the HNC approximation using the effective binary interaction in Eq. (8) and with the Debye form

$$g_{ii}^{\text{DH}}(r) = \exp \left[\frac{-\bar{Z}e^2}{r} e^{-r/\lambda_D} \right], \quad (16)$$

where

$$\lambda_D^{-2} = 4\pi n_e e^2 (\bar{Z} + 1) \beta. \quad (17)$$

g_{ii}^{DH} shows the tendency of the DH approximation to

TABLE I. Summary of selected neon plasma conditions described by the models. \bar{Z} is the mean charge per ion. Γ is the ion-coupling parameter.

Electron density (cm ⁻³)	Temperature (eV)	\bar{Z}	Γ
10 ²⁴	400	8.77	2.2
2 × 10 ²⁴	250	7.61	3.4
5 × 10 ²⁴	250	7.85	4.9
5 × 10 ²⁵	210	8.02	13.1

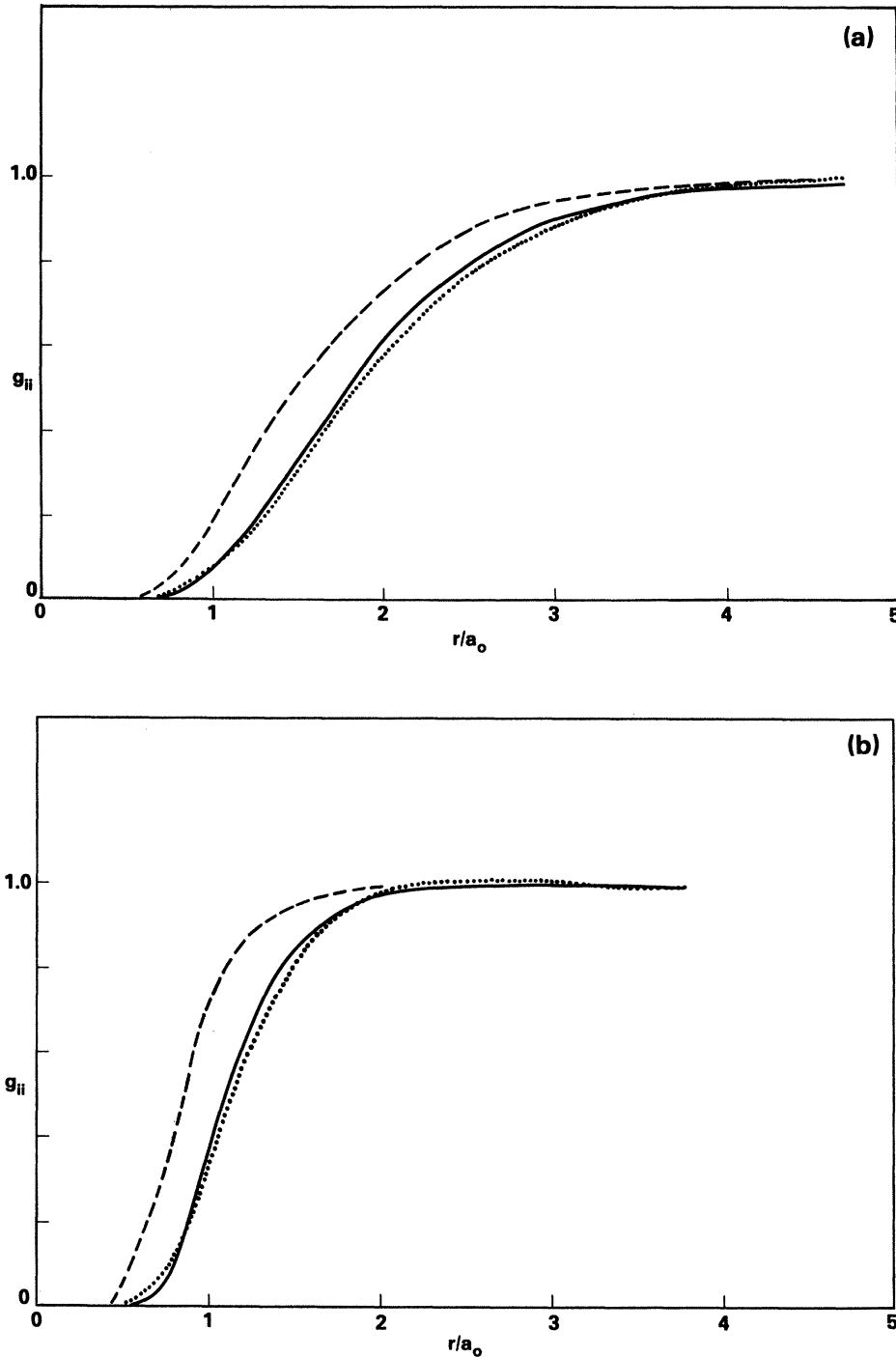


FIG. 1. Ion-ion radial distribution functions for (a) $\Gamma=2.2$ and (b) $\Gamma=4.9$ in HNC (dotted curve), SC (solid curve), and DH (dashed curve) approximations. Distance r is in units of the Bohr radius a_0 .

excessively screen the ions in dense plasma, an effect previously seen in the one-component plasma^{9,20} (OCP) and the two-component plasma (TCP).¹⁴ The HNC RDF is assumed to be the most accurate of the three representations because, since $\lambda_{ii}/r_0 \simeq 10^{-5}$, the ions are essentially classical particles and the computer simulations have supported the use of the HNC approximation for classical systems. In spite of the fact that ρ_i in the SC method—Eq. (8)—cannot reproduce the oscillations around $g_{ii} = 1.0$

for $2 \lesssim r/a_0 \lesssim 4$ in the larger Γ case, the agreement between the SC and HNC methods even at $\Gamma=4.9$ is very good. The small difference between these two forms is not expected to alter the effective potential,²¹ we will test the significance of the difference below.

Figure 2 compares the electron density profile (including both bound and free electrons) provided by the self-consistent method around an ion with the ion-electron radial distribution function produced by the HNC code for

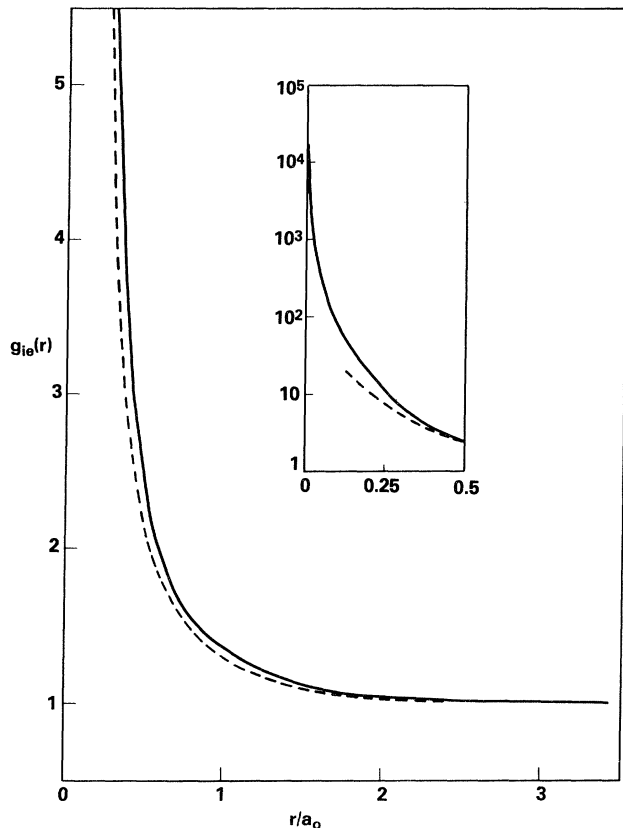


FIG. 2. Electron distribution around an ion for $\Gamma=2.2$. Solid curve is the SC model, dashed curve is the HNC approximation. Smallest radius used in the Fourier transform within the HNC scheme was $r/a_0=0.125$

$\Gamma=2.2$. The profiles are very close for $r/a_0 \gtrsim 0.25$. The innermost r point calculated on the Fourier transform mesh in the HNC code is $r/a_0=0.125$. This also corresponds to the innermost r mesh point of the potential; since $V(r=0)/e^2=Z$, interpolation between $r=0$ and the first mesh point is possible for $V_{\text{HNC}}(r)$. Extrapolation of the HNC g_{ie} to smaller radii, however, would not be meaningful, since $\lambda_{ie}/a_0=0.12$; thus quantum-mechanical details are important in this region. Rogers has investigated this subject for hydrogen, as well as few-times ionized argon and xenon.¹⁶ Since our goal is a many-body effective potential with which to examine average atom calculations, we find that the present model is adequate.

The SC effective potential is a consequence of the solution of the model. This function in the form $rV(r)$ appears in Fig. 3 for $\Gamma=2.2$ and 4.9. The HNC-Poisson potential—Eq. (14)—is also presented. The two forms are seen to be very similar in both cases, indicating the apparent validity of the quantum-mechanical model even at very high densities. The Debye potential reveals much stronger screening except for large distances where $rV(r)$ tends to 0 for all models.²² The ion-sphere approximation is included for comparison. It agrees rather well with the SC and HNC-Poisson methods at short distances, but predicts even larger than Debye screening farther as r becomes larger—a tendency very much distinct from the SC

and HNC methods. The overall form of the IS function is very different from the exponential behavior of the DH, SC, and HNC-Poisson functions, a result of its constraint of fixed ionic volume.

Having now seen that the self-consistent formalism can provide reasonable charge distributions and potentials (compared with the HNC data) for these strongly coupled plasmas, we now look at the energy levels of the neon ions. Table II is a compilation of negative energy eigenvalues arising from the solution of the Schrödinger equation—Eq. (3)—within the method. All negative (bound) energies are noted. The less deeply bound or absent DH values (resulting from more severe screening) as well as eigenvalues found by using $V_{\text{IS}}(r)$ and $V_{\text{HNC}}(r)$ are presented for comparison.

As a test of the significance of the difference between the two forms of the ion-distribution functions—the SC [Eq. (7)] and HNC [Eq. (9)]—a run of the SC model was repeated for $\Gamma=3.4$ using g_{ii}^{HNC} as a fixed function instead of Eq. (7). Those figures are set in parentheses in Table II. The difference is indeed minor and of the order of the numerical accuracy of the coded formalism.

As an example of neon plasma at extreme conditions, we examined the case in which $n_e=5 \times 10^{25} \text{ cm}^{-3}$ and $T=210 \text{ eV}$, giving a Γ of 13.1. In this regime one expects to see considerable difference between the profiles produced by the SC and HNC methods. In Fig. 4 the ion distributions of the HNC, SC, and DH theories are reproduced. The HNC RDF shows that in this case ion correlations are not Boltzmann-like. The non-negligible oscillation about $g_{ii}=1$ shows that there is now a strong indication of ion ordering. Since the SC method utilizes Eq. (7), this effect is not seen in those results. Quantitatively the SC and HNC RDF's are more dissimilar than the less-coupled cases, although the DH curve is considerably more distinct from both of these.

Figure 4 indicates that the effects of non-Boltzmann ion correlations are expected to be seen in the potential only at distances of r/a_0 greater than 1. Inside this radius the SC and HNC ion distributions are similar enough that the potential, which here depends on the electron distribution, is not expected to be greatly affected. The Debye potential is expected again to be overly screened. Figure 5 provides the calculated potentials for $\Gamma=13.1$. The ordering seen in Fig. 5 is obviously manifested as the r -space oscillations in $V(r)$. For purposes of atomic calculations, this effect will have little significance as the spatial extent of the $1s$ wave function is limited to the volume inside $r/a_0=0.15$. For comparison we have plotted the ion-sphere potential (crosses), which is seen to coincide closely with the SC and HNC effective potentials up to $r/a_0=0.5$.

IV. DISCUSSION

Our primary goal is to investigate the applicability of the SC quantum statistical method to strongly coupled neon plasmas. As points of comparison we include potential calculations from Debye-Hückel and ion-sphere approximations. The solution to the HNC equations incorporating a semiclassical binary pseudopotential,¹³ which

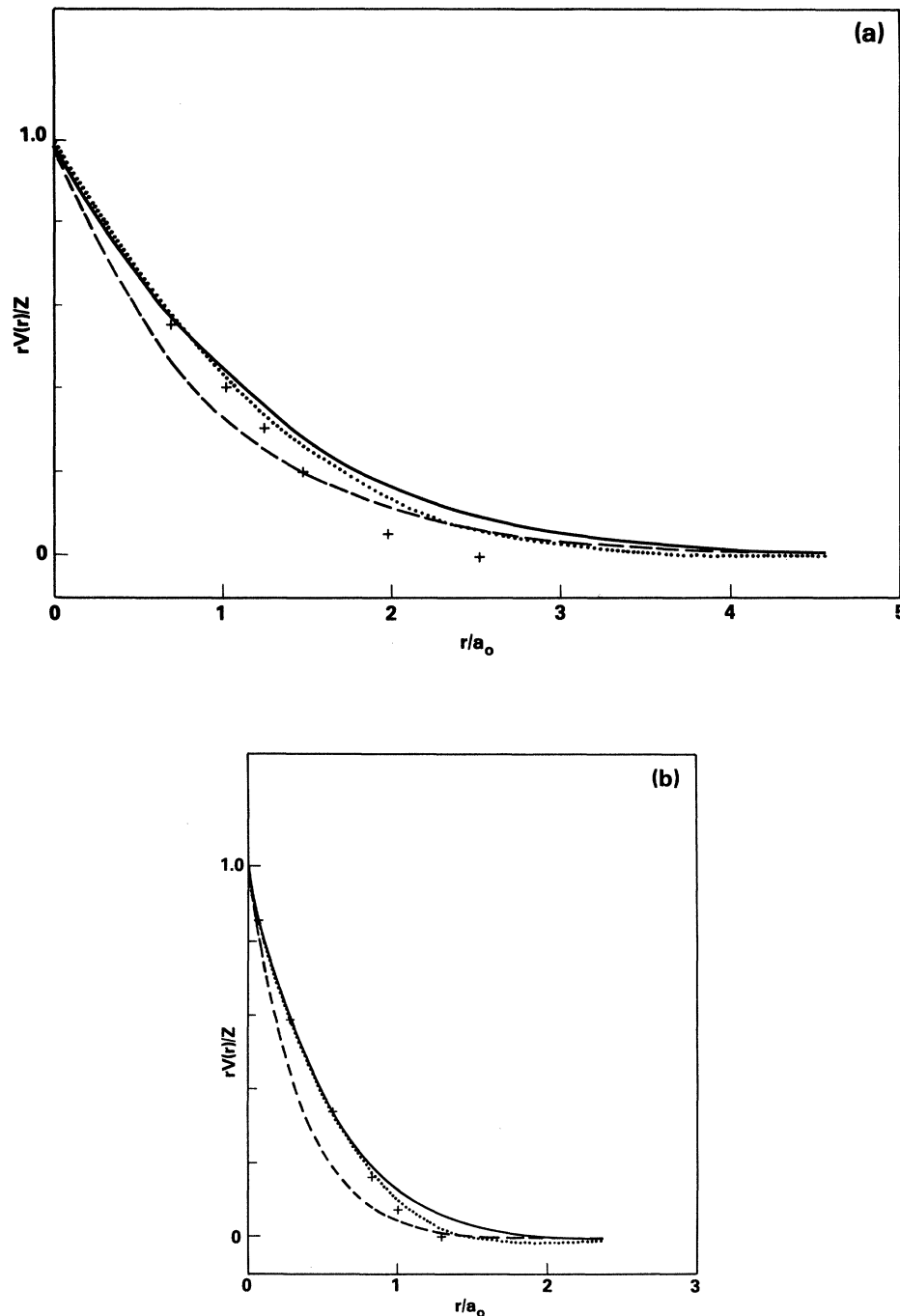


FIG. 3. Effective electron-ion potential resulting from the SC model (solid curve), HNC-Poisson model (dotted curve), ion-sphere model (crosses), and DH theory (dashed curve) for (a) $\Gamma=2.2$ and (b) $\Gamma=4.9$.

has been found to be accurate in strongly coupled hydrogen plasmas,¹⁴ is the plasma model whose statistical properties the SC method must mirror in order to be considered valid in this regime.

The SC method incorporates ion correlations via a Boltzmann factor with the self-consistent potential in the exponent. Although this form is approximate and cannot predict strong correlations which result in spatial oscillations in g_{ii} , the SC ion distribution is very close to the HNC profile for all cases considered, with the exception

of $\Gamma=13$. The DH profiles predict more closely packed ions due to considerably more screening. The IS form is nearly correct for $\Gamma=13$ ($r_0=0.64a_0$). Of course the structural oscillations are absent in the IS model but this should not be very important for calculations involving only bound electrons.

The SC potential is found to be very similar to $V_{\text{HNC}}(r)$ for the lower Γ cases. The HNC potential is less screened than the SC potential in the region $r < r_0/2$, where the electron distribution essentially determines the form of the

TABLE II. Energy eigenvalues in atomic units of neon plasmas at $\Gamma=2.2, 3.4, 4.9,$ and 13.1 from self-consistent model (using g_{ii}^{HNC} in place of ρ_i^{SC} for the parenthetical values under $\Gamma=3.4$), and the HNC-Poisson model, Debye model, and ion-sphere model predictions. All bound-level energies are given.

	$\Gamma=2.2$				$\Gamma=3.4$			
	SC	HNC	IS	DH	SC	HNC	IS	DH
$1s$	-42.3	-43.1	-43.8	-39.7	-34.6 (-34.6)	-39.4	-41.8	-33.7
$2s$	-6.15	-6.35	-6.45	-4.40	-2.88 (-2.89)	-3.77	-4.65	-1.54
$2p$	-5.93	-6.24	-6.40	-4.00	-2.31 (-2.41)	-3.41	-4.55	-0.77
$3s$	-0.64	-0.57	-0.23	-0.16				
$3p$	-0.50	-0.44	-0.12	-0.01				
$3d$	-0.22	-0.18						
	$\Gamma=4.9$				$\Gamma=13.1$			
$1s$	-31.4	-34.1	-39.0	-25.8	-20.0	-21.5	-27.1	-0.66
$2s$	-1.30	-1.14	-2.40					
$2p$			-2.13					

potential. The SC electron distribution and thus the effective potential in this region are probably more accurate than the HNC results. For larger r , however, the ion distribution begins to effect the potential. The ion-ion RDF curves in Figs. 1 and 4 show the ions generally less packed in the HNC approximation than in the SC method, but the structure is not simple. The enhanced (non-Boltzmann-like) ion correlations shorten the range of the calculated potential. The HNC potential in this region is probably the more accurate of the two.

Figure 5 indicates the presence of very strong enhanced correlations affecting the potential. Using the HNC ion distributions in the SC method in place of the Boltzmann

form does not allow $g_{ii}(r)$ to adjust to changes in the electron distribution in each iteration (unless the two-component HNC code is coupled directly to the SC scheme, a project we have not undertaken). Only for large Γ might this be important. For bound-state energies at $\Gamma=13$, the differences between the HNC and SC potentials are not important (see Table II). Calculations of continuum potentials will, however, be affected. This problem will be investigated in the future.

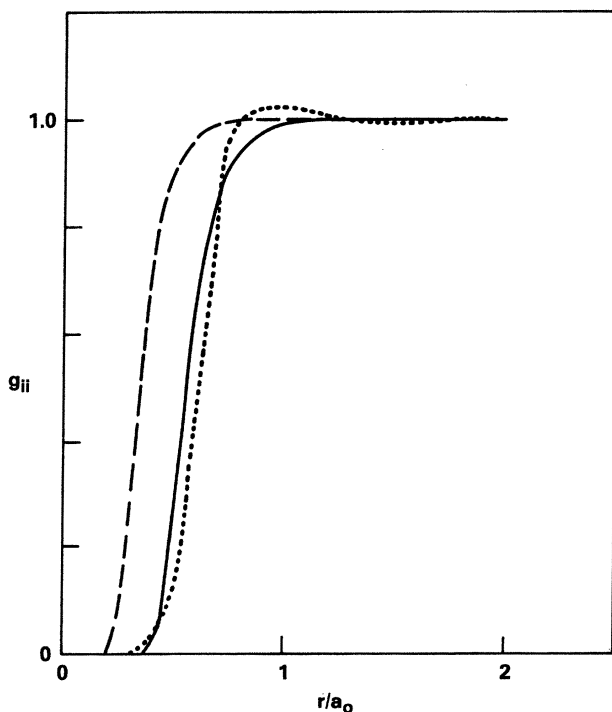


FIG. 4. Ion-density distribution function for the $\Gamma=13.1$ case in three approximations. Symbols are the same as in Fig. 1.

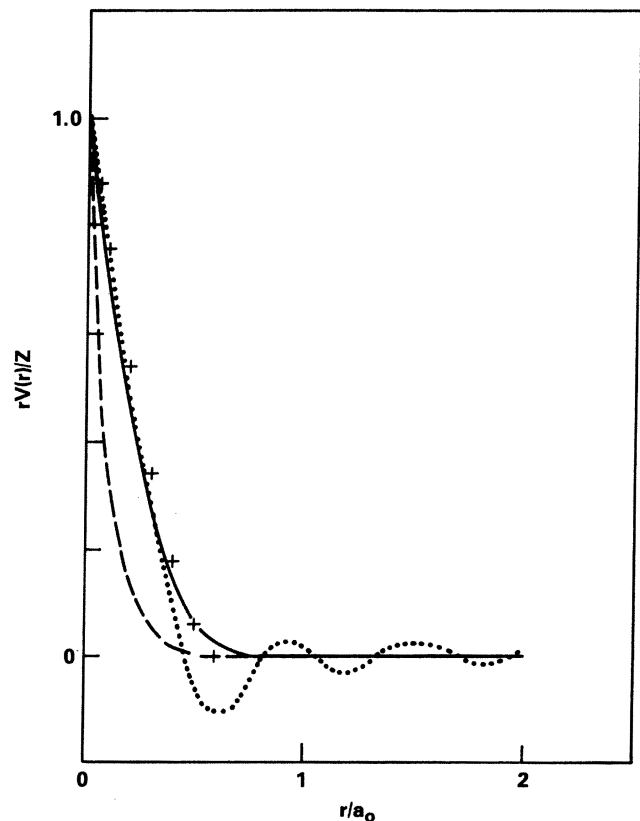


FIG. 5. Effective electron-ion potential for $\Gamma=13.1$ neon. Symbols are identical to Fig. 3.

The inner region is more important for obtaining information on bound states. Here, the ion-sphere approximation is hampered by the assumption of uniform electron density, with the result that $V_{IS}(r)$ predicts more deeply bound state than the HNC or SC potentials (which are in turn more deeply bound than the inappropriate DH values). This is true even at the extreme case of $\Gamma=13.1$ as indicated by Table II. At the temperatures and densities for the cases listed, the HNC and SC potentials predict the same number of bound states with approximately the same energies. The IS approximation predicts more deeply bound inner levels but may result in less energetically bound outer levels (as in $\Gamma=2.2$) if the wave functions extend into the region where the range of the IS potential is foreshortened by its definition of a fixed ionic volume. The Debye values all indicate more shallow states because of large screening. [If in the definition of λ_D in Eq. (17) Z were used instead of \bar{Z} , the result would be even more severe screening. Setting $\bar{Z}=0$ in Eq. (17), i.e., using the electron Debye length, produces a potential devoid of any ionic contributions to the correlation functions. The result here is a potential that lies much above all of the curves; this approximation provides too little screening.]

Since the HNC-Poisson potential appears to be accurate for atomic calculations in neon for $\Gamma < 2.2$ (see Fig. 3 and Table II), this approximation, which is very easy to generate, can be used to examine other properties of such strongly coupled systems requiring a many-body potential. For calculations at higher coupling and details of electron distributions very close to the nucleus, the self-consistent method is needed.

We have shown the self-consistent model produces reliable results for strongly coupled plasmas compared to hypernetted-chain results in neon up to Γ of order 5 and higher if HNC ion distributions are employed. In addition, we have shown that the HNC method of generating correlation functions provides an effective potential that can be used in calculations of atomic properties up to Γ of order 2 (for neon). Debye-Hückel theory is not a mean-

ingful approximation in strongly coupled plasmas. Nor can we recommend the use of the ion-sphere potential for any of the cases examined here.

ACKNOWLEDGMENTS

The authors would like to thank Forrest Rogers for helpful discussions. This work was supported in part by the U.S. Office of Naval Research.

APPENDIX

Here we briefly discuss the use of Z (and not \bar{Z}) in the definition of V_{HNC} . The mean charge \bar{Z} is used in the HNC model to find the charge distributions which define V_{HNC} .

Close to a test point ion of charge \bar{Z} , the free-electron distribution determines $V_{HNC}(r)$; the ion-ion RDF is negligible out to a distance of about $\frac{1}{2}r_0$. In this region Poisson's equation is

$$\nabla^2 V'_{HNC}(r) = 4\pi e^2 \bar{Z} \left[\delta(r) - \frac{n_e}{\bar{Z}} h_{ie}(r) \right], \quad r < r_0/2 \quad (A1)$$

where the primes on $V_{HNC}(r)$ indicates the test ion has charge \bar{Z} , not Z . For a given temperature and electron density, a higher value of \bar{Z} simply pulls the electron distribution $h_{ie}(r)$ in tighter, an effect that essentially compensates the \bar{Z} prefactor to h_{ie} . The result is that the function in parentheses in Eq. (A1) is nearly insensitive to the mean ionic charge, i.e.,

$$V'_{HNC}(r) = 4\pi e^2 \bar{Z} f(r), \quad (A2)$$

where $f(r)$ is a function nearly independent of \bar{Z} . This is the rationale behind the form of the potential in Eq. (13); $V_{HNC}(r)$ is a screening function dependent on density and temperature scaled by the nuclear charge Z . We find that this form very nearly reproduces the potentials found in the quantum-mechanical self-consistent model described earlier.

¹R. M. More, in *Applied Atomic Collision Physics*, edited by H. S. Massey (Academic, New York, 1983), Vol. II.
²J. C. Weisheit, in *Applied Atomic Collision Physics*, edited by H. S. Massey (Academic, New York, 1983), Vol. II.
³R. D. Cowan and J. Ashkin, *Phys. Rev.* **105**, 144 (1957).
⁴B. F. Rozsnyai, *Phys. Rev. A* **5**, 1137 (1972).
⁵S. Skupsky, *Phys. Rev. A* **21**, 1316 (1980).
⁶J. Davis and M. Blaha, *Physics of Electronic and Atomic Collisions*, edited by S. Datz (North-Holland, New York, 1982).
⁷U. Gupta and A. K. Rajagopal, *Phys. Rep.* **87**, 259 (1982).
⁸U. Gupta, M. Blaha, and J. Davis (unpublished).
⁹J. P. Hansen, *Phys. Rev. A* **8**, 3096 (1973).
¹⁰M. Baus and J. P. Hansen, *Phys. Rep.* **59**, 1 (1980); S. Ichimaru, *Rev. Mod. Phys.* **54**, 1017 (1982).
¹¹U. Gupta and A. K. Rajagopal, *Phys. Rev. A* **22**, 2064 (1980).
¹²M. W. C. Dharma-wardana and R. J. Taylor, *J. Phys. C* **14**, 629 (1981).

¹³C. Deutsch, *Phys. Lett.* **60A**, 317 (1977).
¹⁴J. P. Hansen and I. R. McDonald, *Phys. Rev. A* **23**, 2041 (1981).
¹⁵J. F. Springer, M. A. Pokrant, and F. A. Stevens, Jr., *J. Chem. Phys.* **58**, 4863 (1973).
¹⁶F. Rogers, *Phys. Rev. A* **29**, 868 (1984).
¹⁷R. Kubo, *J. Phys. Soc. Jpn.* **12**, 570 (1957).
¹⁸R. M. More, in *Proceedings of Atomic and Molecular Processes in Controlled Fusion*, edited by C. J. Joachain and D. E. Post (Plenum, New York, 1983).
¹⁹M. W. C. Dharma-wardana and F. Perrot, *Phys. Rev. A* **16**, 344 (1982).
²⁰S. G. Brush, H. L. Sahlin, and E. Teller, *Phys. Rev.* **45**, 2102 (1966).
²¹M. W. C. Dharma-wardana, *J. Quant. Spectrosc. Radiat. Transfer* **27**, 315 (1982).
²²See, e.g., Fig. 1 of Ref. 6 for comparison.